



HAL
open science

Analysis of Hybrid Broadcast/Broadband Networks With Multiple Broadcasting Stations

Ahmad Shokair, Matthieu Crussière, Jean-Francois Helard, Youssef Nasser,
Oussama Bazzi

► **To cite this version:**

Ahmad Shokair, Matthieu Crussière, Jean-Francois Helard, Youssef Nasser, Oussama Bazzi. Analysis of Hybrid Broadcast/Broadband Networks With Multiple Broadcasting Stations. IEEE Access, 2019, 7, pp.141226-141240. 10.1109/ACCESS.2019.2942139 . hal-02432461

HAL Id: hal-02432461

<https://univ-rennes.hal.science/hal-02432461>

Submitted on 7 Jul 2020

HAL is a multi-disciplinary open access archive for the deposit and dissemination of scientific research documents, whether they are published or not. The documents may come from teaching and research institutions in France or abroad, or from public or private research centers.

L'archive ouverte pluridisciplinaire **HAL**, est destinée au dépôt et à la diffusion de documents scientifiques de niveau recherche, publiés ou non, émanant des établissements d'enseignement et de recherche français ou étrangers, des laboratoires publics ou privés.



Distributed under a Creative Commons Attribution 4.0 International License

Received April 28, 2019, accepted September 5, 2019, date of publication September 18, 2019, date of current version October 9, 2019.

Digital Object Identifier 10.1109/ACCESS.2019.2942139

Analysis of Hybrid Broadcast/Broadband Networks With Multiple Broadcasting Stations

AHMAD SHOKAIR^{1,3}, MATTHIEU CRUSSIÈRE¹, JEAN-FRANCOIS HÉLARD¹,
YOUSSEF NASSER², AND OUSSAMA BAZZI³

¹INSA -Rennes, IETR, 35700 Rennes, France

²ECE Department, American University of Beirut, Beirut 1107, Lebanon

³Department of Physics and Electronics, Faculty of Science 1, Lebanese University, Hadath 1106, Lebanon

Corresponding author: Ahmad Shokair (ashokair@insa-rennes.fr)

This work was supported by the French state granted to the Convergence TV project through the 20th FUI (transverse inter-ministry funding) program.

ABSTRACT Hybrid broadcast/broadband network (HBBN) presents a potential solution to mitigate the increasing demand for mobile TV. A proper HBBN deployment alleviates the limitations that each standalone network faces, thereby enhancing the global network coverage and efficiency. In this paper, we propose to address the question of performance improvement expected from such HBBN by means of an analytical framework based on stochastic geometry modeling. To this end, we introduce a generic model of the HBBN where multiple broadcast transmitters and a broadband network are deployed in the same area, jointly offering linear services, one of the mobile TV services. Two different approaches derived from stochastic geometry are applied and compared through the analysis of what is commonly referred to as a Point Hole Process (PHP): Original Poisson Point Process (PPP), and reduced PPP. Both approaches are thoroughly analyzed to give better insights into broadcast/broadband coexistence while taking into account the inter-cell interference of both networks. Exact and simplified expressions for the key performance metrics are derived such as the probability of coverage and ergodic capacity. Those expressions are then used to numerically maximize the spectral and power efficiency of the HBBN regarding the broadcast coverage radius and transmitters' density. The results show that for a wide range of user density, the HBBN introduces gain compared to either BB or BC networks. To the best of the authors' knowledge, this paper presents the first work dealing with the optimization of HBBN based on such a generic model and taking inter-cell and inter-network interference into consideration.

INDEX TERMS Access network cooperation, DVB-T2, hybrid networks, LTE, mobile TV, network planning, stochastic geometry.

I. INTRODUCTION

The demand for mobile TV has been expanding during the past few years, following the increasing availability of smartphones and tablets [1]. From the other side, this growth in the usage of such devices and services is leading to an excessive load on the broadband (BB) spectral resource thus creating the so-called spectrum crisis. One sector of mobile TV is linear services, where the transmitter fully controls the stream. Even though the non linear services (YouTube, Netflix...) are growing fast, linear services remain a crucial part of the experience, especially for live data, like breaking news,

The associate editor coordinating the review of this manuscript and approving it for publication was Jesús Hamilton Ortiz.

sports events, musical concerts... While the broadcast (BC) networks present a good solution to deliver these services, their high power consumption reduces their efficiency especially if the number of users drops. A hybrid approach has recently emerged as a possible solution to meet the demand for such resource-hungry TV services. The aim of this paper is to investigate in which extend such hybrid approach can bring any improvement in the service delivery efficiency by setting up a generic broadcast/broadband network model based on stochastic geometry and upon which key performance metrics are derived and analyzed. In that respect, we first present the state-of-the-art solutions for the delivery of linear services followed by the available cooperation hybrid approaches.

A. LINEAR MOBILE TV SERVICE

The mobile TV market recorded a 7.69 billion US dollars revenue in 2015 and is expected to reach 17.02 billion US dollars by 2024 [1], [2]. Practically, so-called linear service is a one type of mobile TV which may be delivered to a mobile terminal by both BC and BB networks.

One of the most known BC solutions today is provided by the Digital Video Broadcast (DVB) project that includes many standards, namely with the 2nd generation of terrestrial digital BC standard (DVB-T2), designed to serve both fixed and mobile users [3]. More recently, the Advanced Television System Committee released the specifications of its 3rd generation standard (ATSC-3.0), also targeting fixed as well as mobile devices [4]. With their high-power transmission towers and mutual spectrum usage among users, BC networks are very efficient in serving a large number of endpoints. Nonetheless, such benefits are partly scaled down in mobility scenarios in an environment where the number of users is variable. A reduction in the number of interested users will make the BC loose its primary advantage, and the cost of high power consumed is not rewarded with high throughput anymore. [5].

BB networks can also deliver mobile TV, but using a different strategy compared to BC networks. BB networks covers large service areas divided into relatively small cells with relatively low transmission power. In each cell, service delivery is conventionally carried out using the Unicast (UC) mode in which the spectrum resource is shared and distributed to users [6]. With unicast, BB networks are very efficient to individualize the service delivery but may suffer from overload issues when a large number of users are demanding for high bandwidth services [7]. Alternatively multicast capabilities may also be exploited to benefit from a mutual resource exploitation through the Evolved Multimedia Broadcast Multicast Services (eMBMS) that was embedded in the Long Term Evolution (LTE) standard [8], [9]. However, this latter mode can only be deployed within a limited number of networks around the world. In such mode, the network will reserve certain number of resource blocks for the shared transmission, reducing the available spectrum for other users.

B. HYBRID NETWORKS AND RELATED WORKS

The limitations discussed above of both conventional BC and BB networks drew attention towards a hybrid solution where a BB network and a BC network collaborate to deliver linear services. This kind of hybrid network could be seen as an offload of the data traffic from the limited BB network to the BC network where the spectral resources are mutualized. It can also be considered as an extension of the coverage range of mobile TV BC with the aid of the widely deployed BB network.

The Hybrid Broadcast Broadband Network (HBBN) approach has recently driven numerous studies in the literature. The importance of the idea and the possible challenges and opportunities were discussed in [5], [10], [11]. An HBBN

can take different forms, like stream sharing networks where BB and BC share the communication chain while each performs certain jobs, and user sharing networks where BB and BC serve different subsets of users.

Stream sharing hybrid networks were studied in the literature from different perspectives, like load switching in [12], push-based content delivery in [13], and 3D media delivery and its business model in [14]. Moreover, a unified physical layer was discussed in [15] and a Cloud Radio Access Network (C-RAN) based cooperative architecture was introduced in [16]. However, this type of hybrid networks requires deep modifications in at least one of the layers of the serving networks.

Hence, our interest in this paper is more focused on user sharing networks. A first stand-alone DVB-NGH and LTE model was presented in [17]. The authors in [18] derived a theoretical analysis of the coverage of hybrid BC/UC networks and concluded that an optimal point of operation leading to maximum HBBN capacity could be found. Complementary to that, a closed-form expression for the ergodic capacity of such HBBN was derived in [19] in the case of non-cooperative interfering coexistence between the BC and UC components. Following this non-cooperative strategy, we recently introduced a hybrid model with a single BC transmitter covering the central part of a service area, and the UC base stations (BSs) covering the rest of that area [20]. Therein, the average probability of coverage, the ergodic capacity achieved by such network was analytically derived. The obtained results are however limited to the case of a single BC station. This paper aims at providing much more generic results on HBBN performance by introducing and dealing with a generic HBBN model made of multiple BC and multiple BB stations.

C. IMPORTANCE OF STOCHASTIC GEOMETRY MODELING

From all these works, it turns out that the evaluation of the potential gains expected from such HBBN requires a thorough analysis based on realistic network models.

Stochastic geometry has provided a realistic description of the cellular network compared to a grid model [21], [22]. In such an approach, a Poisson Point Process (PPP) is used to model the positions of the BSs in the network. Stochastic geometry provides suitable mathematical tools to analyze the network's performance. The network is described by a single parameter that represents the density of the BSs. Several studies have since then been conducted using such approach [23]. The accuracy of the model was compared with the real network UK case study in [24]. It was shown that the PPP model, and even if it gives slightly lower coverage values than the real implementation, is still more accurate and tractable than conventional grid model [25]. Stochastic geometry has also been used in the context of broadcasting like in [26]. Despite the importance of this analysis, the hybrid existence still needs a thorough investigation mainly in a multi-cell environment. By averaging over the whole area,

stochastic geometry can obviously describe the mobile nature of users.

D. CONTRIBUTIONS AND ORGANIZATION

In this paper, a user sharing HBBN with multiple Broadcast Transmitters (BCTs) is proposed and analyzed using stochastic geometry. It is assumed that the BB component of the HBBN implements UC delivery mode. Multicast is disregarded in this work since it inherits lots of the drawbacks of BC, and since standards like eMBMS are not widely deployed. Moreover, it was shown in a previous work that high coverage could be achieved with UC if a proper resource allocation is used [6].

Unlike previous works that discuss heterogeneous and multi-tier networks (such as in cellular), this paper focuses on the nature of the broadcast service. Indeed, contrary to other services, BC is characterized by the pre-fixed rates while the design is based on the worst case user service. The importance of our work resides in the consideration of the Inter-Cell Interference (ICI) in the network optimization as it represents a major factor affecting the quality of service of such hybrid network but was neglected in previous works such as [7], [18], [27]. Moreover, this work gives great insights and conclusions of this hybrid existence model as: (i) it considers the coexistence between the two services over the same frequency band causing mutual interference, (ii) it simplifies the user association to either network (BC or BB) to have much simpler expressions, and (iii) takes the nature of the service into account when calculating the system rate and efficiency. To the best of the authors' knowledge, this is the first contribution of its kind in which a realistic model with interference consideration both between cells and between networks is adopted using stochastic geometry. The main contributions of this paper could be summarized as follows:

- Proposition of a user sharing HBBN model where the BC and the BB networks share the same band.
- Inclusion and analysis of ICI as a major factor in the design of the HBBN. Here, ICI of both networks is considered. The interference due to coexistence between the two networks is also studied.
- Derivations of the novel analytical expressions of the average probability of coverage for UC, BC, and any user in the service area, as well as the average normalized capacity for those cases, using stochastic geometry tools for modeling and analysis, with two approaches for simplification: normal and reduced PPP.
- Optimization of the HBBN by maximizing selected evaluation metrics like the probability of coverage, spectral efficiency, and power efficiency, in terms of the main design parameters such as the density of BCT and the size of the BC zone represented by the BC radius.

The rest of this paper is organized as follows. Section II describes the network architecture and provides the derivation of some important probability distribution functions (PDF). Sections III and IV include the derivation of the average coverage probability and its respective upper and lower bounds.

Average user capacity, system capacity, and power efficiency are analyzed in V. In section VI, numerical simulations are conducted. Then, a set of parameters is optimized aiming at maximizing the coverage and rate. Finally, section VII draws the conclusions of the paper.

II. MODEL DESCRIPTION

In this section, the proposed model of the hybrid network is first presented and then followed by the main derivations used in the next sections. For simplicity, the used annotations are summarized in Table 1.

TABLE 1. Used symbols.

Symbol	Parameter
M, N, K	Average number of users, BS, BCTs
Ψ, Φ, Ξ	PPP of users, BS, BCTs
$\lambda_U, \lambda_{BS}, \lambda_{BC}$	Density of users, BS, BCTs
P_L, P_D	Isotropic Tx power from BS and BCTs
P_n	Rx noise power
g, h	Channel between a user and BCT, BS
μ, τ	Rates of g and h
$I_{U/B}, F$	Interference on BC user from BS, BCT
$I_{U/U}, I_{B/U}$	Interference on UC user from BS, BCT
r_b	Broadcast radius
$\alpha \beta$	Pathloss exponent for UC, BC
T_{bc}, T_{uc}	SINR threshold for BC and UC
r_v	Distance from BC user to serving BCT.
r_s	Distance from BC user to interfering BS
r_t	Distance from BC user to other BCT
r_l	Distance from UC user to serving BS
r_q	Distance from UC user to interfering BS
r_d	Distance from UC user to interfering BCT
P_{UC}, P_{BC}	Probability for a user to be in UC, BC

A. SYSTEM DESCRIPTION

This work considers the delivery of TV linear services to an average of M users, distributed uniformly over the service area according to a PPP Ψ with density λ_U . The users are served by one of the two networks:

- Broadband UC network: it consists of number of BSs uniformly distributed over the service area according to a PPP Φ with density λ_{BS} . The BSs are transmitting Orthogonal Frequency-Division Multiplexing (OFDM) data with isotropic power P_L .
- Broadcast network: it consists of an average of K BCTs, uniformly distributed over the service area with another PPP Ξ with a density λ_{BC} , which is much smaller than λ_{BS} . The BCTs are broadcasting OFDM data with isotropic power P_D , where $P_D > P_L$. Normally, BCT are not modeled by random processes, since their positions are often well planed, but future networks -as the model presented herein- can be more dense, and therefore a PPP may accurately describe the network deployment, while bringing in the advantage of making the analysis tractable.

An example of the service area is shown in Fig. 1. The coverage area for the BCT is larger than that of the BSs due to a larger transmitted power. To simplify the analysis procedure, it is assumed that a BCT has a circular coverage area centered at the BCT and with radius r_b . Any user within any of the BC areas is served by the nearest BCT. The users that are not covered by any of the BC areas are served by the nearest BS.

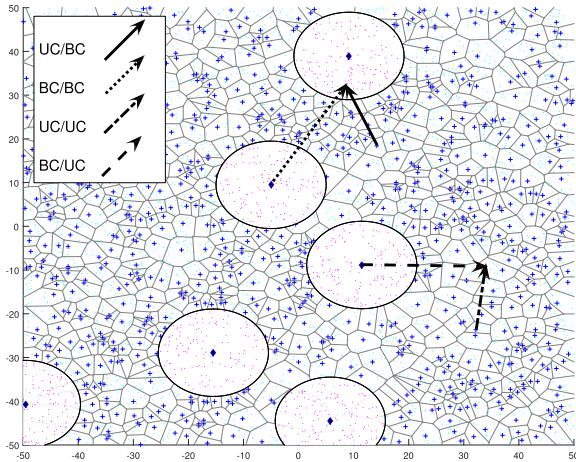


FIGURE 1. An example of a service area, with $\lambda_{BC} = \lambda_{BS}/200$ and with $r_b = 10$ km. The discs are the BC zones (with BCTs in the middle), and the boxes with Voronoi tessellation are UC cells, with BS in the middle of each (distances are in km).

In this work, it is assumed that the BCTs operate at frequency f_D . The UC BSs outside the BC covered areas also operate at the same frequency f_D , while the UC BSs located within any of the BC areas operate at frequency f_L . Those BSs are not transmitting linear services and will have no role in our model, and they will not cause any interference to other parts of the system. Even though such coexistence between two networks is not currently implemented, such deployment may be a solution for a better usage of the spectrum. The TV white space or the unlicensed bands can be the domain where such coexistence can take place. On the other side, since all the BSs (outside of the BCTs’ areas) and all the BCTs operate at the same frequency, a mutual interference will be created between the two networks that have to be quantified and evaluated. In fact, one of the key technological bottlenecks in this work is to optimize the service area of the BCTs, among others. Within this context, 4 types of signals have to be considered:

- Interference to BC users:
 - from UC BSs (UC/BC called hereafter $I_{U/B}$): BC users within the coverage area of the BCT still receive a certain amount of power from all the outside BS operating at the same frequency. This interference will be especially significant for the BC edge users.
 - Power from other BCTs (BC/BC named F): In this paper, we use the Single Frequency Network (SFN) configuration to minimize the utilization of

the spectrum despite the need to synchronize all the BCTs (out of the scope of this paper). The received power is partially useful and will be added to the received signal. This will be detailed later.

- Interference to UC users:
 - Interference from other UC BSs (UC/UC named $I_{U/U}$), or ICI: this type of interference is the most severe since the interfering BSs are relatively close to the users.
 - Interference from BCTs (BC/UC $I_{B/U}$): the BC power leaked to the surrounding UC users, especially those who are close to the BC zones, is seen as interference signal since BCTs and BSs are not synchronized.

B. SINR DEFINITION

The Signal to Interference and Noise Ratio (SINR) is calculated for each system. For a typical BC user, we define the SINR as follows:

$$S_{bc} = \frac{P_D g r_v^{-\beta} + \gamma F}{P_n + I_{U/B}} \tag{1}$$

where P_D represents the transmitted power by the BCT, g is a random variable that represents the random behavior of the BC channel and has an exponential distribution, i.e. $g \sim \exp(\tau)$ with τ being the rate of the distribution, r_v represents the distance between the user and the serving BCT, β is the path loss exponent for BC transmission, γ is a weighting factor for the usefulness of the received BC power and it will be discussed later, and P_n is the noise power. $I_{U/B}$ is defined as follows:

$$I_{U/B} = \sum_{n \in \mathcal{N}} P_L h_n r_{s_n}^{-\alpha} \tag{2}$$

where \mathcal{N} is the set of all UC BSs, r_{s_n} is the distance between the user and the n^{th} interfering UC BS, h is a random variable that represents the random behavior of the UC channel and has an exponential distribution, i.e. $h \sim \exp(\mu)$, and here h_n refers to the channel between the user and the n^{th} interfering BS. α is the path loss exponent for UC transmission.

On the other hand, F is the summation of all received signals from other BCTs. According to [28], due to multiple received signals with different arrival times from SFN transmitters, the received signal from a transmitter falls under one of the following cases:

- The received signal delay vs the transmission time is less than the guard interval. In this case, all received power is useful.
- The delay is larger than the guard interval but smaller than the total symbol time (symbol time+guard interval): portion of the power is useful and the other is interference.
- The delay is larger than the total symbol duration, and thus all the received power is seen as interference.

The third case happens when the distance between the SFN transmitter and receiver is very large. Hence, the received

power is very small, so it will not be included in our SINR expression. Even though it is well known that the non-useful power is counted as interference, but due to the small effect of such interference compared to other interference sources, it is neglected in the SINR definition we have introduced in (1) for simplification. The first two cases are approximated and modeled by a weighting factor $0 \leq \gamma \leq 1$ of the total received power F as an approximation to simplify the analysis. The latter is defined as:

$$F = \sum_{k \in \mathcal{K} \setminus i} P_D h_k r_{ik}^{-\beta} \quad (3)$$

where $\mathcal{K} \setminus i$ is the set of all BCT, excluding the serving BCT. r_{ik} h_k is the distance and channel from the BC user to the k^{th} BCT respectively.

For a typical UC user, the SINR is given by:

$$S_{uc} = \frac{P_L h r_l^{-\alpha}}{P_n + I_{U/U} + I_{B/U}} \quad (4)$$

where r_l is the distance between the user and the serving BS, and $I_{U/U}$ is the total interference received by a UC user from the interfering BS, given by:

$$I_{U/U} = \sum_{n \in \mathcal{N} \setminus j} P_L h_n r_{qn}^{-\alpha} \quad (5)$$

where $\mathcal{N} \setminus j$ is the set of all UC BSs excluding the serving BS, r_{qn} is the distance between the user and the n^{th} interfering UC BS. In addition, $I_{B/U}$ is defined by:

$$I_{B/U} = \sum_{k \in \mathcal{K}} P_D h_k r_{dk}^{-\beta} \quad (6)$$

where r_{dk} is the distance from the k^{th} BCT. One can notice that the SINR models for both BC and UC look similar, but differences exist in the magnitude of the interference, pathloss exponent and transmitted power.

C. PROBABILITY DISTRIBUTION OF THE LINK DISTANCE

Two essential Probability Density Functions (PDFs) must be calculated: (i) the PDF of r_v , the distance between a BC user and the serving BCT, and (ii) the PDF of r_l , the distance between a UC user and its serving BS.

The distribution of r_v needs more effort to be obtained so it will be discussed first. The related PDF is stated in the following Lemma.

Lemma 1: Considering a HBBN with multiple BCTs each having a circular coverage area with radius r_b , the PDF of the distance r_v between a typical BC user and its serving BCT is:

$$f_{r_v}(r_v) = \frac{2\pi \lambda_{BC} r_v \exp(-\lambda_{BC} \pi r_v^2)}{1 - \exp(-\lambda_{BC} \pi r_b^2)} \quad (7)$$

Proof:

$$\mathbb{P}[(r_v > R_v) | BC \text{ user}] = \frac{\mathbb{P}[(r_v > R_v) \cap BC \text{ user}]}{P_{BC}} \quad (8)$$

The probability of a user to be within a BCT area, i.e. BC user, is to have a BCT with a distance smaller than r_b away. It is given by the complementary of the void probability of the BC PPP:

$$P_{BC} = 1 - \exp(-\lambda_{BC} \pi r_b^2) \quad (9)$$

Now, the probability of a user to be a BC user and with distance $r_v > R_v$ is the probability that there is no BCT closer to that user than R_v , and that there is at least one BCT in the strip between the circle of radius R_v and the circle with radius r_b . This probability is given by:

$$\begin{aligned} \mathbb{P}[(r_v > R_v) \cap BC] &= \exp(-\lambda_{BC} \pi R_v^2) (1 - \exp(-\lambda_{BC} \pi (r_b^2 - R_v^2))) \\ &= \exp(-\lambda_{BC} \pi R_v^2) \exp(-\lambda_{BC} \pi r_b^2) \end{aligned} \quad (10)$$

substituting (9) and (10) in (8) gives the CCDF of r_v , and differentiating it will give the PDF stated in (7). ■

On the other hand, the PDF of r_l has been discussed in several previous works addressing stochastic geometry based network models. Starting from the fact that the null-probability of a PPP in \mathbb{R}^2 in an area A is $\exp(-\lambda A)$, the PDF of r_l is given by [21]:

$$f_{r_l}(r_l) = 2\pi r_l \lambda_{BS} \exp(-\lambda_{BS} \pi r_l^2) \quad (11)$$

III. PROBABILITY OF COVERAGE

The probability of coverage is defined as the probability of a user having SINR that exceeds a certain threshold T . However, since the structure of the network is complicated, some approximations can be used to reduce the complexity of the derived formula. In fact, both UC BSs and BCTs are distributed according to a PPP, and the (UC/UC) interference is generated by the whole UC PPP except the gaps generated by BC areas in the interference points. For that reason, the UC network can be seen as a Poisson Hole Process (PHP) [29]. Analyzing PHP can be done with different approaches. One approach is to consider the PHP as a new PPP with reduced density [21]. Another approach is to ignore the holes completely, leading to a lower bound for the probability of coverage by overestimating the interference [30]. In this section, the derivation for the general probability of coverage for BC and UC users is detailed. The general expressions of the Laplace Transform (LT) of the interference are also calculated.

A. GENERAL EXPRESSIONS FOR THE PROBABILITY OF COVERAGE

Let us first derive the probability of coverage $P_{c/BC}$ for BC users. It is defined as the average probability that the SINR for a BC user S_{bc} is greater than a certain threshold T_{bc} . It can be expressed in the following lemma.

Lemma 2: The average probability of coverage $P_{c/BC}$ for BC users is given by:

$$P_{c/BC} = \frac{2\pi\lambda_{BC}}{1 - \exp(-\lambda_{BC}\pi r_b^2)} \int_0^{r_b} r_v \exp(-\pi\lambda_{BC}r_v^2) \exp\left(\frac{-\tau T_{bc}r_v^\beta P_n}{P_D}\right) \mathcal{L}_{I_{U/B}}\left(\frac{\tau T_{bc}r_v^\beta}{P_D}\right) \mathcal{L}_F\left(\frac{-\tau\gamma r_v^\beta}{P_D}\right) dr_v \quad (12)$$

where T_{bc} is the SINR threshold for acceptable coverage in BC, and $\mathcal{L}(\cdot)$ denotes the LT operator.

Proof: See Appendix A

The derived expression in Lemma 2 averages the probability of coverage over two random components of the SINR: the random channel, and the random relative position of the user, i.e. the random distances to BSs and BCTs. Therein we are following the conventional approach found in literature [25]. The first LT corresponds to the interference power from UC BSs on the BC users, and the second LT corresponds to the received power from other BCTs. Expressions for both LTs are derived in the coming sections.

For UC users, the probability of coverage $P_{c/UC}$ has a similar definition as that of BC users, but using a dedicated threshold T_{uc} . This leads to the following Lemma 3.

Lemma 3: The average probability of coverage $P_{c/UC}$ of a UC user is as follows:

$$P_{c/UC} = 2\pi\lambda_{BS} \int_0^\infty r_l \exp(-\pi\lambda_{BS}r_l^2) \exp\left(\frac{-\mu T_{uc}r_l^\alpha P_n}{P_L}\right) \times \mathcal{L}_{I_{U/U}}\left(\frac{-\mu T_{uc}r_l^\alpha}{P_L}\right) \mathcal{L}_{I_{B/U}}\left(\frac{-\mu T_{uc}r_l^\alpha}{P_L}\right) dr_l \quad (13)$$

where T_{uc} is the SINR threshold for sufficient signal reception quality in UC.

Proof: Same steps as for BC users.

Also for UC users, the probability of coverage is averaged over the random channel effect and the relative position of the users. The first LT corresponds to the interference power transmitted by the interfering UC BSs, while the second LT corresponds to the interference conducted by all the BCTs. Even though the two expressions for the probability of coverage for BC and UC users are not in closed forms, the integration is fairly straightforward since most of the LT expressions are in well tabulated special functions.

Finally, for a general user randomly positioned in the service area, the probability of coverage P_c can be seen as the linear combination between probabilities $P_{c/BC}$ and $P_{c/UC}$ previously calculated. This result is stated in Corollary 1.

Corollary 1: The probability of coverage for a general user randomly located in the service area is as follows:

$$P_c = (1 - \exp(-\lambda_{BC}\pi r_b^2))P_{c/BC} + \exp(-\lambda_{BC}\pi r_b^2)P_{c/UC} \quad (14)$$

Proof: The total probability of coverage for a given user is given by:

$$P_c = P_{BC}P_{c/BC} + P_{UC}P_{c/UC} \quad (15)$$

where P_{BC} is the probability that a user is within a broadcast domain, and P_{UC} is the probability that a user is not in any BC domain. P_{BC} is as shown in (9), and P_{UC} is its complementary. Substituting both in (15) gives (14). ■

B. GENERAL EXPRESSIONS OF THE LT OF THE INTERFERENCE

As it can be seen from (12) and (13), the main terms to be considered are the four LTs of the interference. The complexity of those terms determines the complexity of the overall coverage probability. A general term can be found for several cases of the LT and stated in Theorem 1.

Theorem 1: The general expression for an interference sourced from a homogeneous PPP Ω of density λ , starting from a distance d from the user, where the interference is given by:

$$I = \sum Plr^{-\delta} \quad (16)$$

and where P is the transmission power, l is the channel with exponential distribution of rate ρ , r represents the distance, and δ denotes the path loss exponent, is given by:

$$\mathcal{L}_I(s) = \exp\left(\frac{-2\pi\lambda d^{2-\delta} sP}{\rho(\delta-2)} {}_2F_1\left(1, 1 - \frac{2}{\delta}; 2 - \frac{2}{\delta}; \frac{-sP}{\rho d^\delta}\right)\right) \quad (17)$$

where ${}_2F_1(\cdot)$ is the Gaussian hyper-geometric function.

Proof:

$$\begin{aligned} \mathcal{L}_I(s) &= \mathbb{E}_{\Omega, l}[\exp(-sI)] \\ &= \mathbb{E}_{\Omega, l}[\exp(-s \sum_{n \in \mathcal{N}} Pl_n r_n^{-\delta})] \\ &= \mathbb{E}_{\Omega, l}[\prod_{n \in \mathcal{N}} \exp(-sPl_n r_n^{-\delta})] \\ &\stackrel{(a)}{=} \mathbb{E}_{\Omega}[\prod_{n \in \mathcal{N}} \mathbb{E}_l[\exp(-sPl_n r_n^{-\delta})]] \\ &= \mathbb{E}_{\Omega}[\prod_{n \in \mathcal{N}} \frac{1}{1 + \frac{sP}{\rho r_n^\delta}}] \\ &\stackrel{(b)}{=} \exp\left(-\lambda \int_{\mathbb{R}^2} \frac{1}{1 + \frac{\rho r^\delta}{sP}}\right) \\ &\stackrel{(c)}{=} \exp\left(\frac{-2\pi\lambda}{\delta} \int_{d^\delta}^\infty \frac{x^{\frac{2}{\delta}-1}}{1 + \frac{\rho}{sP}x} dx\right) \end{aligned} \quad (18)$$

where (a) follows the independence of the point distribution and the channel effect, and (b) follows Campbell's theorem of the product over a PPP [21]. The integral in (b) is applied on the whole 2-D plane starting at a distance d from the serving point. This results in (c) where the coordinates are switched to polar system, and by substituting $x = r^\delta$. Now using equation 3.194 from [31] that states that:

$$\int_w^\infty \frac{x^{u-1}}{(1+\beta x)^v} dx = \frac{w^{u-v}}{\beta^v(v-u)} {}_2F_1\left(v, v-u; v-u+1; -\frac{1}{\beta w}\right) \quad (19)$$

to solve the integral, $\mathcal{L}_I(s)$ is reduced into (17) ■

The result expression introduced in Theorem 1 is fairly simple, and includes a single tabulated special function that can be quickly evaluated numerically. The problem turns out then to derive the expressions of the LTs of the interference and added power of the HBBN as detailed below.

C. EVALUATION OF THE LTS OF THE BC SIGNALS

The target here is to give the LTs of the BC signals, i.e. F and $I_{B/U}$ as they are easily deduced from Theorem 1. The LT of F on a BC user is independent from the BB network, and thus is independent from the BS density. It is given by the following corollary.

Corollary 2: The LT of the additional received BC power by BC users can be expressed as:

$$\mathcal{L}_F\left(\frac{-\tau\gamma r_v^\beta}{P_D}\right) = \exp\left(\frac{2\pi\lambda_{BC}\gamma r_v^2}{\beta-2} {}_2F_1\left(1, 1-\frac{2}{\beta}; 2-\frac{2}{\beta}; \gamma\right)\right) \quad (20)$$

Proof: Since the received power is due to the BCT distribution, and knowing that the nearest source is r_v away, the general formula introduced in Theorem 1 can be used. Starting from the definition of the added power in (1), and substituting $s = \frac{-\tau\gamma r_v^\beta}{P_D}$, the expression in (20) is obtained. ■

The problem turns out to find the LT of BCT interference on UC users, i.e. $I_{B/U}$. It is given by the following corollary.

Corollary 3: The LT of the interference originated by the BCT on a UC user is expressed as:

$$\mathcal{L}_{I_{B/U}}\left(\frac{\mu T_{uc} r_l^\alpha}{P_L}\right) = \exp\left(-\frac{2\pi\lambda_{BC}\mu P_D T_{uc} r_b^{2-\beta} r_l^\alpha}{\tau P_L(\beta-2)} {}_2F_1\left(1, 1-\frac{2}{\beta}; 2-\frac{2}{\beta}; -\frac{P_D\mu r_l^\alpha T_{uc}}{P_L\tau r_b^\beta}\right)\right) \quad (21)$$

Proof: The interference is originated by a PPP modeling of the BCTs, and since the user is served by UC, then the nearest interference source is at least beyond the distance r_b , then the expression derived in (17) also applies here. By using the interference definition in (6), and with substituting $s = \frac{\mu T_{uc} r_l^\alpha}{P_L}$, the expression in (21) is obtained. ■

IV. SIMPLIFIED EXPRESSIONS OF THE PROBABILITY OF COVERAGE

The expressions of the LTs given in (20) and (21) are easily handled. However, this is not the case for BS interference signals $I_{U/B}$ and $I_{U/U}$ in (12) and (13), which makes the probability of coverage expression harder to evaluate. To simplify the problem, we adopt two different approaches for these interference terms, detailed next.

A. APPROACH 1: EVALUATION OF THE LTS OF THE BS INTERFERENCE USING A REDUCED PPP

As mentioned earlier, the PPP of the UC network with density λ_{BS} can be seen as a PHP due to the void areas created by the BC zones. In this approach, the PHP is approximated

by a new PPP with a reduced density λ'_{BS} (approximation 1). It gives an underestimate for the interference, since in the new reduced-density area all the interfering BSs are farther on average. Hence, the probability of coverage will be over-estimated (upper-bound). The new density λ'_{BS} is given by:

$$\lambda'_{BS} = \lambda_{BS} e^{-\lambda_H \pi r_b^2} \quad (22)$$

A complete derivation of this can be found in III-B in [29].

Let us first start with the case of the UC BS interference on BC users, i.e. $I_{U/B}$. Since the distance from the nearest interfering BS is not fixed, and since the density of the interference sources is not constant in the area around the user because of the random relative position of the user, the derived final expression in (17) can't be used. However, a similar approach for the derivation can be made and yields the following result of Lemma 4.

Lemma 4: Assuming a reduced density PPP model for the UC network of a HBBN with multiple BC stations, the LT of interference of UC BSs on BC users is as follows:

$$\begin{aligned} \mathcal{L}_{I_{U/B}}^u\left(\frac{\tau T_{bc} r_v^\beta}{P_D}\right) &= \exp\left(\lambda'_{BS} \int_{r_b-r_v}^{r_b+r_v} \frac{2r_s \cos^{-1}\left(\frac{r_s^2-r_v^2-r_b^2}{2r_s r_v}\right)}{1 + \frac{\mu P_D r_s^\alpha}{\tau P_L T_{bc}}} dr_s\right) \\ &\exp\left(-\frac{2\pi\lambda'_{BS}\tau P_L T_{bc}(r_b-r_v)^{2-\alpha}}{\mu P_D(\alpha-2)} {}_2F_1\left(1, 1-\frac{2}{\alpha}; 2-\frac{2}{\alpha}; \frac{-P_L\tau T_{bc}}{P_D\mu(r_b-r_v)^\alpha}\right)\right) \end{aligned} \quad (23)$$

The superscript u stands for upper-bound.

Proof: See Appendix B ■

The derivation is done by calculating the interference produced by the entire service area, then subtracting the interference from the BC zone (as it does not cause interference), hence the additional exponential term in the expression.

Now we focus on the LT of UC BS interference on UC users, i.e. $I_{U/U}$.

Corollary 4: Starting from approximation 1, the LT of the interference of UC BS transmission on the UC users is given by:

$$\mathcal{L}_{I_{U/U}}^u\left(\frac{\mu T_{uc} r_l^\alpha}{P_L}\right) = \exp\left(-\frac{2\pi\lambda'_{BS} r_l^2 T_{uc}}{\alpha-2} {}_2F_1\left(1, 1-\frac{2}{\alpha}; 2-\frac{2}{\alpha}; -T_{uc}\right)\right) \quad (24)$$

Proof: Due to PPP modeling and since the nearest interference source is at least at distance r_l (the serving distance), Theorem 1 applies. Starting from the definition of the interference stated in (5), and setting $s = \frac{\mu T_{uc} r_l^\alpha}{P_L}$, the expression in (24) is obtained. ■

B. APPROACH 2: EVALUATION OF THE LTS OF THE BS INTERFERENCE BY IGNORING GAPS

In this approach, the gaps (areas) of the BB interference sources are completely ignored, i.e. the interferers are

considered to be in the whole plane (approximation 2). This will overestimate the interference, and thus give a lower bound for the probability of coverage for BC, UC, and general users. Here, the analytical derivations are the same as with approach one, but with one minor change: the density of the original PPP is used instead of the modified density, i.e. λ_{BS} instead of λ'_{BS} .

Corollary 5: Based on the second approach, the LT of the interference sourced by the BB network on a BC user is expressed as:

$$\mathcal{L}_{I_{U/B}}^l\left(\frac{\tau T_{bc} r_v^\beta}{P_D}\right) = \exp\left(\lambda_{BS} \int_{r_b-r_v}^{r_b+r_v} \frac{2r_s \cos^{-1}\left(\frac{r_s^2-r_v^2-r_b^2}{2r_s r_v}\right)}{1 + \frac{\mu P_D r_s^\alpha}{\tau P_L T_{bc}}} dr_s\right) \exp\left(-\frac{2\pi\lambda_{BS}\tau P_L T_{bc}(r_b-r_v)^{2-\alpha}}{\mu P_D(\alpha-2)}\right) {}_2F_1\left(1, 1-\frac{2}{\alpha}; 2-\frac{2}{\alpha}; \frac{-P_L\tau T_{bc}}{P_D\mu(r_b-r_v)^\alpha}\right) \quad (25)$$

The superscript l stands for lower-bound.

The same applies for $I_{U/U}$ by changing λ'_{BS} to λ_{BS} :

Corollary 6: Starting from the second approximation by ignoring the gaps in the BB network, the LT of the inter-cell interference of UC BSs on a UC user is as follows:

$$\mathcal{L}_{I_{U/U}}^l\left(\frac{\mu T_{uc} r_l^\alpha}{P_L}\right) = \exp\left(\frac{2\pi\lambda_{BS} r_l^2 T_{uc}}{\alpha-2} {}_2F_1\left(1, 1-\frac{2}{\alpha}; 2-\frac{2}{\alpha}; -T_{uc}\right)\right) \quad (26)$$

C. EVALUATION OF THE UPPER AND LOWER BOUNDS OF THE COVERAGE PROBABILITY

As mentioned earlier, the expressions of the probability of coverage for BC and UC users in (12) and (13) respectively are too complicated if the LT terms are to be evaluated exactly. However, the two approximations allow less complex expressions, that correspond to a lower and upper bounds of the interference terms.

Theorem 2: The upper bound of the probability of coverage for the BC user is given by:

$$P_{c/BC}^u = \frac{2\pi\lambda_{BC}}{1 - \exp(-\lambda_{BC}\pi r_b^2)} \int_0^{r_b} r_v \exp(-\pi\lambda_{BC}r_v^2) \exp\left(\frac{-\tau T_{bc} r_v^\beta P_n}{P_D}\right) \mathcal{L}_{I_{U/B}}^u\left(\frac{\tau T_{bc} r_v^\beta}{P_D}\right) \mathcal{L}_F\left(\frac{-\tau\gamma r_v^\beta}{P_D}\right) dr_v \quad (27)$$

and the upper bound of the probability of coverage for UC users is given by:

$$P_{c/UC}^u = 2\pi\lambda_{BS} \int_0^\infty r_l \exp(-\pi\lambda_{BS}r_l^2) \exp\left(\frac{-\mu T_{uc} r_l^\alpha P_n}{P_L}\right) \times \mathcal{L}_{I_{U/U}}^u\left(\frac{-\mu T_{uc} r_l^\alpha}{P_L}\right) \mathcal{L}_{I_{B/U}}\left(\frac{-\mu T_{uc} r_l^\alpha}{P_L}\right) dr_l \quad (28)$$

Proof: In the first approximation, the PHP is approximated by a PPP with a reduced density. The reduction in density means that the point process will be stretched, interfering points will be further away from the user in all directions. Assuming the actual interference to be:

$$I^{actual} = \sum_{n=1}^{N_{BS}} P_l r_{a,n}^{-\delta} \quad (29)$$

where $r_{a,n}$ is the actual distance from the n^{th} interferer, and the calculated interference to be:

$$I^{calc} = \sum_{n=1}^{N_{BS}} P_l r_{c,n}^{-\delta} \quad (30)$$

where $r_{c,n}$ is the calculated distance from the n^{th} interferer, and since in both cases the size of the sum and the transmission power is the same, and the channel is similar with the same distribution and rate, the only difference lies in the distance. Because of the approximation by changing the density and the expansion of the PPP, the calculated distance will on average be higher than the actual one:

$$r_c > r_a \implies I^{calc} < I^{actual} \implies \mathcal{L}_{I_{U/U}}^u(s) > \mathcal{L}_{I_{U/U}}(s)$$

and since the rest of the terms in the coverage probability expressions are the same, then $P_{c/UC}^u$ provides an upper limit for the coverage probability. ■

Theorem 3: The lower bound of the probability of coverage for the BC user can be written as:

$$P_{c/BC}^l = \frac{2\pi\lambda_{BC}}{1 - \exp(-\lambda_{BC}\pi r_b^2)} \int_0^{r_b} r_v \exp(-\pi\lambda_{BC}r_v^2) \exp\left(\frac{-\tau T_{bc} r_v^\beta P_n}{P_D}\right) \mathcal{L}_{I_{U/B}}^l\left(\frac{\tau T_{bc} r_v^\beta}{P_D}\right) \mathcal{L}_F\left(\frac{-\tau\gamma r_v^\beta}{P_D}\right) dr_v \quad (31)$$

and the lower bound of the probability of coverage for UC users can be expressed:

$$P_{c/UC}^l = 2\pi\lambda_{BS} \int_0^\infty r_l \exp(-\pi\lambda_{BS}r_l^2) \exp\left(\frac{-\mu T_{uc} r_l^\alpha P_n}{P_L}\right) \times \mathcal{L}_{I_{U/U}}^l\left(\frac{-\mu T_{uc} r_l^\alpha}{P_L}\right) \mathcal{L}_{I_{B/U}}\left(\frac{-\mu T_{uc} r_l^\alpha}{P_L}\right) dr_l \quad (32)$$

Proof: In this approximation, the gaps are ignored. This leads to count more BSs as interfering sources than the actual number. Denote the actual interference by:

$$I^{actual} = \sum_{n=1}^{N_{BS}^{actual}} P_l r_n^{-\delta} \quad (33)$$

and denote the calculated interference in this approximation by:

$$I^{calc} = \sum_{n=1}^{N_{BS}^{calc}} P_l r_n^{-\delta} \quad (34)$$

Since the terms in the sum are always positive, the value of the sum depends on its size. Also because $N_{BS}^{calc} > N_{BS}^{actual}$, then $I^{calc} > I^{actual}$, and consequently:

$$\mathcal{L}_{I_{U/U}}^l < \mathcal{L}_{I_{U/U}} \quad (35)$$

creating a lower bound for the coverage. ■

V. CAPACITY

In this section, we consider the capacity, or the maximum achievable rate. The maximum spectral efficiency is firstly derived. Then, the average capacity of the hybrid network is considered, followed by system capacity and a power efficiency metric.

A. ERGODIC CAPACITY FOR BC, UC, AND GENERAL USERS

The normalized user capacity is related only to the SINR of the received signal. For BC users, it is given by the following lemma.

Lemma 5: The ergodic capacity of a BC user is given by:

$$\begin{aligned} C_{BC} &= \frac{2\pi\lambda_{BC}}{1 - \exp(-\lambda_{BC}\pi r_b^2)} \int_0^{r_b} r_v \exp(-\lambda_{BC}\pi r_v^2) \int_0^\infty \exp\left(\frac{-\tau u r_v^\beta P_n}{P_D}\right) \\ &\times \mathcal{L}_{I_{U/B}}\left(\frac{\tau u r_v^\beta}{P_D}\right) \mathcal{L}_F\left(\frac{\tau \gamma r_v^\beta}{P_D}\right) \frac{1}{\ln(2)(u+1)} dudr_v \quad (36) \end{aligned}$$

Proof: See Appendix C. ■

The LT terms in (36) are the same as in (12), hence they are used in the derivations.

Similarly, the ergodic capacity for UC users can be calculated.

Lemma 6: The ergodic capacity for a UC user is given by:

$$\begin{aligned} C_{UC} &= 2\pi\lambda_{BS} \int_0^\infty r_l \exp(-\lambda_{BS}\pi r_l^2) \int_0^\infty \exp\left(\frac{-\mu u r_l^\alpha P_n}{P_L}\right) \\ &\times \mathcal{L}_{I_{U/U}}\left(\frac{\mu u r_l^\alpha}{P_L}\right) \mathcal{L}_{B/U}\left(\frac{\mu u r_l^\alpha}{P_L}\right) \frac{1}{\ln(2)(u+1)} dudr_v \quad (37) \end{aligned}$$

Proof: Similar steps to that of the BC capacity are followed. ■

The form of (37) is close to that of the probability of coverage for UC users presented in (13), but with one more averaging level. The LT therein can be evaluated using (24) and (21) with a simple change of parameters.

For a general user, the capacity is the combination between the two capacities, given by:

$$C = P_{BC}C_{BC} + P_{UC}C_{UC} \quad (38)$$

B. AVERAGE SYSTEM CAPACITY AND POWER EFFICIENCY

1) TOTAL SYSTEM CAPACITY

The derivations above are given for the average spectral efficiency. However, it is useful to calculate the average system capacity, or the total capacity achieved by all the users in the

service area. The system capacity is the sum of capacities of the two networks, and it could be defined as following:

$$C^{sys} = C_{BC}^T + C_{UC}^T \quad (39)$$

where C_{BC}^T is the total capacity of the BC network and C_{UC}^T is the total capacity of the UC network.

Corollary 7: Following the definition in (39), the system capacity of a hybrid network with multiple BCTs is given by:

$$\begin{aligned} C^{sys} &= A \exp(-\lambda_{BC}\pi r_b^2) C_{UC} \lambda_{BS} N^{RB} B^{RB} \\ &+ \lambda_U A (1 - \exp(-\lambda_{BC}\pi r_b^2)) P_{c,i} C^{req} \quad (40) \end{aligned}$$

where A is the service area, N^{RB} is the total number of resource blocks available for a cell BS, and B^{RB} is the bandwidth of a single resource block.

Proof: The capacity of the UC network is the sum of the UC users' capacities, or the product of the average user capacity and the number of users:

$$\begin{aligned} C_{UC}^T &= M_{UC} C_{UC} B^{user} \\ &= \lambda_U A P_{UC} C_{UC} N^{RB/user} B^{RB} \\ &= \lambda_U A \exp(-\lambda_{BC}\pi r_b^2) C_{UC} \frac{\lambda_{BS}}{\lambda_U} N^{RB} B^{RB} \quad (41) \end{aligned}$$

where B^{user} is the bandwidth allocated to a user, and $N^{RB/user} = \frac{\lambda_{BS}}{\lambda_U} N^{RB}$ is the average number of resource blocks allocated to a user following a uniform allocation for resources. The second step follows the uniform distribution of users, and the final step follows the assumption of a uniform allocation of resource and substituting the UC probability by its expression. As for the total capacity of the BC network, its derivation is done differently. Indeed, as the BCT is broadcasting with a predetermined data rate, the total capacity is the number of connected users multiplied by the predefined rate, which is in this case, the minimum required capacity for a user to be connected (C^{req}):

$$\begin{aligned} C_{BC}^T &= N_U^{BC} C^{req} \\ &= \lambda_U A P_{BC} P_{c/BC} C^{req} \\ &= \lambda_U A (1 - \exp(-\lambda_{BC}\pi r_b^2)) P_{c/BC} C^{req} \quad (42) \end{aligned}$$

Adding the two expressions completes the proof. ■

Note that the the total UC capacity is independent of user density, since the available resources in a cell will be allocated for whatever the number of users would be in that cell. For BC, however, the total capacity depends on the user density, and it is independent of the average user capacity.

2) POWER EFFICIENCY

The power efficiency of the system, or the normalized system capacity is defined as the ratio between the system capacity and the total transmitted power, and is defined as following:

$$\begin{aligned} \eta_P &:= \frac{C^{sys}}{\sum P_D + \sum P_L} \\ &= \frac{\lambda_U P_{BC} P_{c/BC} C^{req} + P_{UC} C_{UC} \lambda_{BS} N^{RB} B^{RB}}{\lambda_{BC} P_D + \lambda'_{BS} P_L} \quad (43) \end{aligned}$$

This metric includes all the important design parameters: the BC radius r_b which is embedded in P_{UC} , P_{BC} , $P_{c/BC}$, and $P_{c/UC}$, the BCT density λ_{BC} , the BS modified density λ'_{BS} , the transmission powers P_D and P_L and also depends on the density of the users in the service area λ_U . In fact, it will be extremely complicated to calculate the optimal operation point directly from this formula. Instead, numerical evaluation of the above equation will be given later for different working conditions.

VI. SIMULATION RESULTS

In this section, numerical evaluations are drawn for a variety of system conditions. The results are divided into three main parts: (1) verification of the derived formulas and approximations by Monte-Carlo (MC) simulations, (2) optimization of the hybrid network in terms of BC radius r_b and density of BCT λ_{BC} .

A. SIMULATION SETTING

The service area is selected to be a square area of side equal to 100 km, with variable BC radius and BC density. Throughout this section, γ is set to 0.8. This value was concluded from simulations based on the model presented in [28] for DVB-T2 in 8 MHz bandwidth and 8K mode (often used for mobile reception) reported in [32]. Default simulation settings are summarized in TABLE 2. These settings will result in a similar deployment as the example in Fig. 1.

TABLE 2. Simulation parameters.

Parameter	Value	Parameter	Value
P_L, P_D (isotropic)	1.2 & 17 kW	r_b	10 km
BW_{BC}, BW_{UC}	8 & 20 MHz	P_n	-100 dBm
α, β	3.4 & 3.2	μ, τ	1 & 1
λ_{BS}, λ_u	0.15, $1/km^2$	N^{RB}	100 RB/cell

B. ANALYTICAL SOLUTIONS AND SIMULATION RESULTS

Therein, the expressions derived in sections III, IV and V are compared to the MC simulation results. Fig 2 shows that the derived formulas for the probability of coverage match perfectly with the simulation results whatever the threshold T

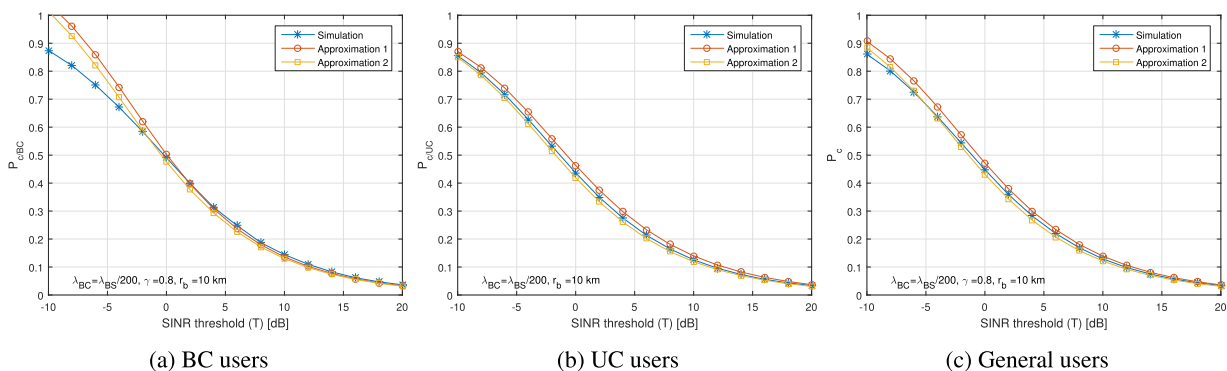


FIGURE 2. P_c for BC, UC and general users for $r_b = 10$ km, $\gamma = 0.8$ and $\lambda_{BC} = \lambda_{BS}/200$.

is, except for very low thresholds for BC users. These limitations were explained through the derivation of the coverage probability in Appendix A. Furthermore, it can be seen that approximation 1 (from expressions (27) and (28)) represents an upper bound while approximation 2 (from expressions (31) and (32)) represents a lower bound for the actual coverage as expected in section III. Both approximations have good accuracy, with an advantage to the lower bound, which almost overlaps the MC simulation results. Here, we omit other cross-checks due to space limitations.

C. OPTIMIZATION OF THE HYBRID NETWORK

In this part, we aim at finding an optimal point of operation for the hybrid network in terms of key design parameters: BC radius r_b , and BCT density λ_{BC} . The metrics used for evaluation are the probability of coverage, the spectral efficiency, and the network power efficiency. Since the derived expressions are proved to be accurate (lower bounds in particular), they will be exclusively used for the rest of the paper.

1) OPTIMIZATION OF COVERAGE

Maximizing the probability of coverage is a key design goal. Fig. 3 shows the average probability of coverage as a function of the BC radius r_b with three different values of user density. The figure shows that an optimal point where the coverage is maximized does exist. In a UC network, higher user density means lower average allocated bandwidth for each user, which will reduce the number of covered users. Then, more contribution is needed from the BC side, which results in a higher optimal r_b .

Fig. 4 shows that increasing the density of BCT enhances the coverage except the case with very low user density, as expected. The higher the number of BCT, the more users are connected to the BC, and because of the relatively higher coverage of the BC, the higher the coverage will be. Moreover, it can be noticed that the rate of growth for the coverage probability increases with the user density of the network. As expected, for low user density, the BB network can handle the service alone, and any additional BCT density will not affect the coverage.

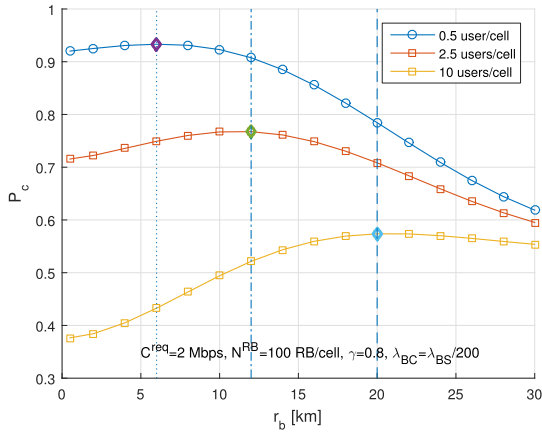


FIGURE 3. Probability of coverage versus the BC radius.

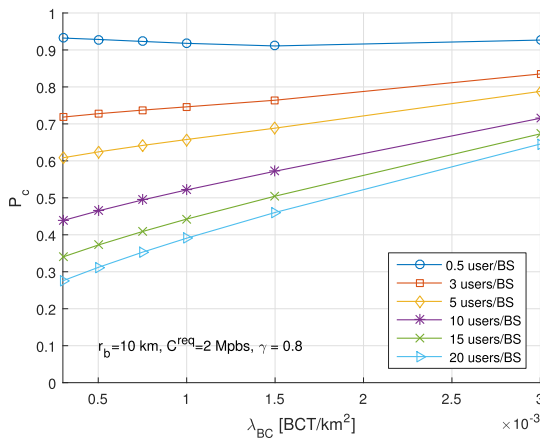


FIGURE 4. Probability of coverage versus the density of BCT.

2) OPTIMIZATION OF SPECTRAL EFFICIENCY

Spectral efficiency gives an indication on the capability of the system to properly use spectral resources. With the limited available band in the BB network, it is important to optimize the spectral efficiency of the hybrid network.

Fig. 5 provides the optimum BC radius that maximizes the average spectral efficiency of the users. Note that the

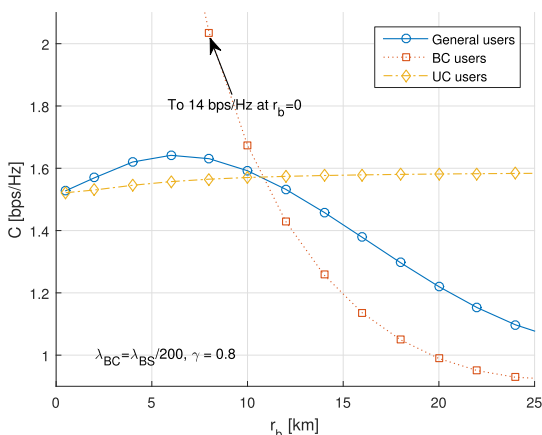


FIGURE 5. Spectral efficiency versus the BC radius.

normalized capacity is independent of the SINR threshold and consequently from user density. Results in Fig. 5 indicate that adding the BC component to a BB network increases the spectral efficiency, especially for users that are within an optimum radius of the BCT (note that $r_b = 0$ corresponds to BB network). However, after a certain point of the BCT radius, the edge users whose number increases with the radius r_b become far from the BCT, and consequently get lower capacity.

For the same BC radius, the effect of BCT density on the spectral efficiency is studied next. Note that the total BC power is maintained, so the transmission power of a single BCT decreases as we increase the BCT density. It can be seen from Fig. 6 that increasing the number of BCTs degrades the BC spectral efficiency. Even though increasing the BCT density will reduce the interference from the UC BSs and enhance the received power for BC users, the reduction in transmission power for each BCT appears to be a dominant factor, therefore reducing the global spectral efficiency. The results show that the best capacity-wise performance is achieved when the density of the BCT is low, in contrary to that of the BB BSs. This indicates that scale diversity of the hybrid approach (combination of the dense and sparse networks) is a key factor in the design.

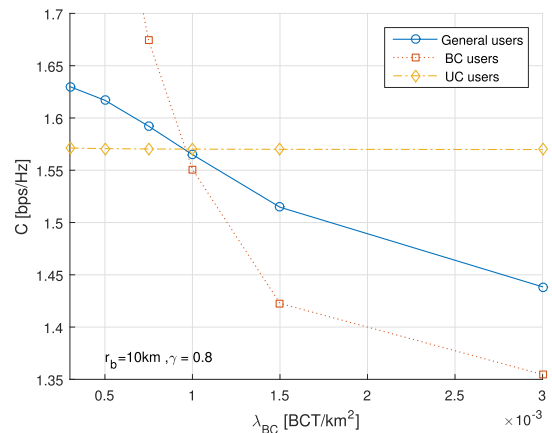
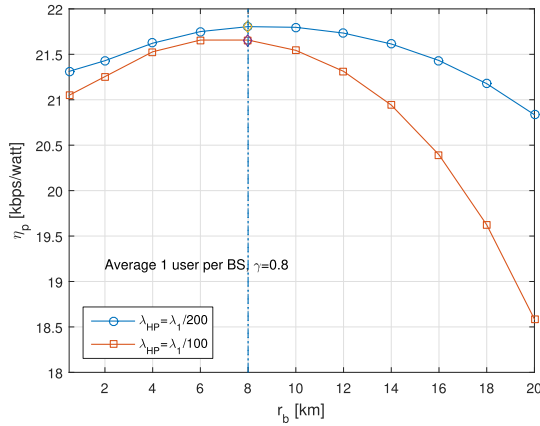


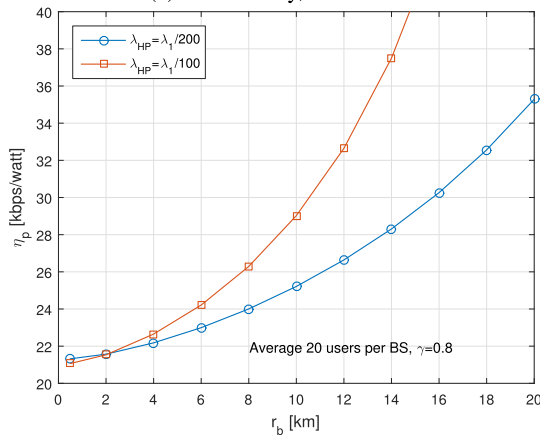
FIGURE 6. Spectral efficiency versus the density of BCT.

3) OPTIMIZATION OF POWER EFFICIENCY

Maximum coverage can theoretically be achieved by covering the whole service area by a large number of BCTs with small BC radius. However, such a solution requires a huge amount of energy, and thus is not feasible. The power efficiency defined in (43) is a suitable metric to assess achievable system capacity taking power consumption into consideration. Fig. 7 illustrates the variation of power efficiency as a function of BC radius for two values of BCT density, and for low and high user density. In a service area with low user density, as shown in Fig. 7a with an average of 1 user per BS (requesting mobile TV service), increasing the BC radius enhances the power efficiency of the network until the optimal radius is reached. Beyond this point, expanding the



(a) Low density, 1 user/BS



(b) High density, 20 users/BS

FIGURE 7. Power efficiency of a service area with $\gamma = 0.8$ and for different loading scenarios.

BC zone will add more edge BC users, without introducing any gain in coverage and capacity, which reduces the power efficiency. In contrary, Fig. 7b shows that for a service area with high user density, higher r_b will always produce greater efficiency, due to the overload on the BB network. Expanding the BC contribution in a user-dense area by rising r_b will

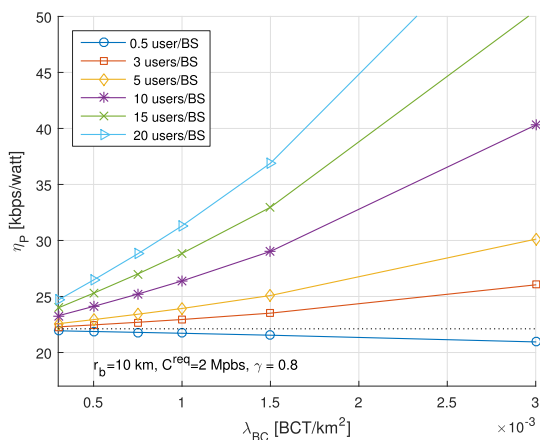


FIGURE 8. Power efficiency of a service area versus BCT density.

take out power consuming UC BSs, and serve more users by including them in the BC network, and consequently increases the efficiency.

Results in Fig. 8 reveal that rising the BCT density affects the power efficiency differently depending on the user density. For low user density (like the curve of 0.5 users/BS), where BB can manage to deliver enough bandwidth to the users, increasing the number of BCTs will add a huge amount of power load without having a significant added value to the coverage and capacity. When the area is dense (like in the curves of 15 and 20 users/BS), adding more BCT will offload the users to the BC network, and take out the BSs because of their excessive power consumption. Consequently, this increases the power efficiency.

VII. CONCLUSION

The demand for mobile TV services is expected to be growing during the next few years while the conventional approaches suffer from several limitations. In this paper, we introduced and evaluated a novel stochastic geometry-based approach for a hybrid BB/BC network, with multiple BCTs distributed over the service area. Therein, two approximations for the obtained PHP were used to simplify the analysis (the original and the modified PPPs) in order to derive the analytical expressions of both the probability of coverage and the spectral efficiency of the users. Moreover, suitable approximations have been derived and verified through extensive MC results. The derived expressions were then used to numerically optimize the hybrid network performance in terms of coverage, spectral efficiency, and power efficiency, as a function of the key design parameters, that is the BC radius and the BCT density. Results showed that the hybrid approach brings in the best performance excluding the extreme cases of a very low and very high number of users. Hereby, it was proved that optimal operating points exist, which are governed by the BC radius and BCT density. This work presented a first of its kind in optimizing such a hybrid solution from different perspectives using stochastic geometry while taking both ICI and inter-network interference into consideration.

APPENDIX A PROOF OF LEMMA 2

For BC network, the probability of coverage is the average probability that the SINR for a BC user S_{bc} is greater than a certain threshold T_{bc} . It can be derived as follows:

$$\begin{aligned}
 P_{c/BC} &= \mathbb{E}_{r_v} \left[\mathbb{P}(S_{bc} > T_{bc} \mid r_v) \right] \\
 &= \mathbb{E}_{r_v} \left[\mathbb{P} \left[\frac{P_D g r_V^{-\beta} + \gamma F}{P_n + I_{U/B}} > T_{bc} \mid r_v \right] \right] \\
 &= \mathbb{E}_{r_v} \left[\mathbb{P} \left[g > \frac{T_{bc} r_V^\beta}{P_D} (P_n + I_{U/B} - \frac{\gamma F}{T_{bc}}) \mid r_v \right] \right] \\
 &= \int_0^{r_b} \mathbb{P} \left[g > \frac{T_{bc} r_V^\beta}{P_D} (P_n + I_{U/B} - \frac{\gamma F}{T_{bc}}) \mid r_v \right] f_{r_v}(r_v) dr_v \quad (45)
 \end{aligned}$$

But

$$\begin{aligned} \mathbb{P}[g > \frac{T_{bc}r_v^\beta}{P_D}(P_n+I_{U/B}-\frac{\gamma F}{T_{bc}}) | r_v] & \quad (46) \\ \stackrel{(a)}{=} \mathbb{E}_{F,I_{U/B}}[\exp(-\frac{\tau T_{bc}r_v^\beta}{P_D}(P_n+I_{U/B}-\frac{\gamma F}{T_{bc}}))] \\ \stackrel{(b)}{=} \exp(-\frac{\tau T_{bc}r_v^\beta P_n}{P_D})\mathbb{E}_{I_{U/B}}[\exp(-\frac{\tau T_{bc}r_v^\beta}{P_D}I_i)] \\ & \quad \times \mathbb{E}_F[\exp(\frac{\tau \gamma r_v^\beta}{P_D}F)] \\ \stackrel{(c)}{=} \exp(-\frac{\tau T_{bc}r_v^\beta P_n}{P_D})\mathcal{L}_{I_{U/B}}(\frac{\tau T_{bc}r_v^\beta}{P_D})\mathcal{L}_F(-\frac{\tau \gamma r_v^\beta}{P_D}) \end{aligned} \quad (47)$$

where $\mathcal{L}(\cdot)$ denotes the LT. (a) is valid if and only if $(P_n + I_{U/B} - \frac{\gamma F}{T_{bc}}) > 0$ and it follows the exponential distribution of the random variable g . In fact, (a) will lose some accuracy when the power from other BCTs is higher than the sum of the noise power and the (UC/UC) interference, and this will happen only when the BCTs are very close to each other, which is not the case in practice. (b) follows the independence between the interference and the useful power, and (c) follows the definition of the LT: $\mathcal{L}_f(s)\mathbb{E}[e^{-sX}]$. Substituting in (44), and replacing $f_{r_v}(r_v)$ by its value provides the final expression.

**APPENDIX B
PROOF OF LEMMA 4**

Let $s_1 = \frac{\tau T_{bc}r_v^\beta}{P_D}$. The first LT can be evaluated as following:

$$\begin{aligned} \mathcal{L}_{I_{U/B}}(s_1) &= \mathbb{E}_{\Phi,h}[\exp(-s_1 I_{U/B})] \quad (48) \\ &= \mathbb{E}_{\Phi,h}[\exp(-s_1 \sum_{n \in \mathcal{N}} P_L h_n r_{s_n}^{-\alpha})] \end{aligned}$$

$$\begin{aligned} &= \mathbb{E}_{\Phi,h}[\prod_{n \in \mathcal{N}} \exp(-s_1 P_L h_n r_{s_n}^{-\alpha})] \quad (49) \\ &\stackrel{(a)}{=} \mathbb{E}_\phi[\prod_{n \in \mathcal{N}} \mathbb{E}_h[\exp(-s_1 P_L h_n r_{s_n}^{-\alpha})]] \end{aligned}$$

$$= \mathbb{E}_\phi[\prod_{n \in \mathcal{N}} \frac{1}{1 + \frac{s_1 P_L}{\mu r_s^\alpha}}] \quad (50)$$

$$\stackrel{(b)}{=} \exp(-\lambda'_{BS} \int_{\mathbb{R}^2 \setminus \mathcal{G}} \frac{1}{1 + \frac{\mu r_s^\alpha}{s_1 P_L}}) \quad (51)$$

where (a) follows the independence of the PPP and the channel, and (b) follows Campbell’s theorem of the product over a PPP. The integral in (b) is applied on the whole 2-D plane excluding the gap created by the absence of any interferer inside the BC zone. The result will then be:

$$\begin{aligned} \mathcal{L}_{I_{U/B}}(s_1) &= \exp\left(-\lambda'_{BS} \int_{r_b-r_v}^{\infty} \frac{2\pi r_s}{1 + \frac{\mu r_s^\alpha}{s_1 P_L}} dr_s\right. \\ & \quad \left. + \lambda'_{BS} \int_{r_b-r_v}^{r_b+r_v} \frac{2r_s \cos^{-1}\left(\frac{r_s^2 - r_v^2 - r_b^2}{2r_s r_v}\right)}{1 + \frac{\mu r_s^\alpha}{s_1 P_L}} dr_s\right) \end{aligned} \quad (52)$$

Substituting s_1 by its value, and applying (19) on the first term gives the final expression as in (23).

**APPENDIX C
PROOF OF LEMMA 5**

starting from the definition of the user capacity, the average capacity of a BC user can be derived as follows:

$$\begin{aligned} C_i &= \mathbb{E}[\log_2(1+S_{bc})] \\ &= \mathbb{E}_{\Phi,g}\left[\log_2\left(1 + \frac{P_D g r_v^{-\beta} + \gamma F}{P_n + I_{U/B}}\right)\right] \\ &= \int_0^{r_b} f_{r_v}(r_v) \mathbb{E}\left[\log_2\left(1 + \frac{P_D g r_v^{-\beta} + \gamma F}{P_n + I_{U/B}}\right) | r_v\right] dr_v \\ &\stackrel{(a)}{=} \int_0^{r_b} f_{r_v}(r_v) \int_0^\infty \mathbb{P}\left[\log_2\left(1 + \frac{P_D g r_v^{-\beta} + \gamma F}{P_n + I_{U/B}}\right) > t | r_v\right] dt dr_v \\ &= \int_0^{r_b} f_{r_v}(r_v) \int_0^\infty \mathbb{P}\left[g > \frac{(2^t - 1)r_v^\beta}{P_D}(P_n + I_{U/B} - \frac{\gamma F}{2^t - 1}) | r_v\right] dt dr_v \\ &= \int_0^{r_b} f_{r_v}(r_v) \int_0^\infty \mathbb{E}_{I_{U/B},F}\left[\exp\left(-\frac{\tau(2^t - 1)r_v^\beta}{P_D}(P_n + I_{U/B} - \frac{\gamma F}{2^t - 1})\right)\right] dt dr_v \end{aligned}$$

where (a) follows from $\mathbb{E}[X] = \int_0^\infty \mathbb{P}(X > x) dx$. Now by substituting $f_{r_v}(r_v)$ by its expression, and substituting $2^t - 1$ by u , the ergodic capacity for BC users will be as in (36).

ACKNOWLEDGMENT

This work has received a French state support granted to the Convergence TV project through the 20th FUI (transverse inter-ministry funding) program. The authors would also like to thank the “Image & Réseaux” and “Cap Digital” French business clusters for their support of this work.

REFERENCES

- [1] *Mobile TV Market (Service-Free to Air Service and Pay TV Service)—Global Industry Analysis, Size, Share, Growth, Trends and Forecast 2016–2024*, Transparency Market Res., New York, NY, USA, 2016.
- [2] C.-H. Wong, G. W.-H. Tan, T.-S. Hew, and K.-B. Ooi, “Can mobile TV be a new revolution in the television industry?” *Comput. Hum. Behav.*, vol. 55, pp. 764–776, Feb. 2016.
- [3] M. El-Hajjar and L. Hanzo, “A survey of digital television broadcast transmission techniques,” *IEEE Commun. Surveys Tuts.*, vol. 15, no. 4, pp. 1924–1949, Apr. 2013.
- [4] L. Fay, L. Michael, D. Gómez-Barquero, N. Ammar, and M. W. Caldwell, “An overview of the ATSC 3.0 physical layer specification,” *IEEE Trans. Broadcast.*, vol. 62, no. 1, pp. 159–171, Mar. 2016.
- [5] H. Voigt, “Hybrid media and tv delivery using mobile broadband combined with terrestrial/satellite tv,” in *Proc. 15th Electron. Conf. Biennial Baltic*, 2016, pp. 1–10.
- [6] A. Shokair, Y. Nasser, O. Bazzi, J.-F. Hélar, and M. Crussière, “Near optimal linear-service oriented resource allocation strategy for LTE networks,” in *Proc. 9th Int. Congr. Ultra Mod. Telecommun. Control Syst. Workshops (ICUMT)*, Nov. 2017, pp. 73–78.
- [7] P.-A. Fam, M. Crussière, J.-F. Hélar, P. Brétilon, and S. Paquelet, “Global throughput maximization of a hybrid unicast-broadcast network for linear services,” in *Proc. Int. Symp. Wireless Commun. Syst. (ISWCS)*, Aug. 2015, pp. 146–150.

- [8] D. Lecompte and F. Gabin, "Evolved multimedia broadcast/multicast service (eMBMS) in LTE-advanced: Overview and Rel-11 enhancements," *IEEE Commun. Mag.*, vol. 50, no. 11, pp. 68–74, Nov. 2012.
- [9] L. Christodoulou, O. Abdul-Hameed, and A. M. Kondo, "Toward an LTE hybrid unicast broadcast content delivery framework," *IEEE Trans. Broadcast.*, vol. 63, no. 4, pp. 656–672, Dec. 2017.
- [10] J. Calabuig, J. F. Monserrat, and D. Gómez-Barquero, "5th generation mobile networks: A new opportunity for the convergence of mobile broadband and broadcast services," *IEEE Commun. Mag.*, vol. 53, no. 2, pp. 198–205, Feb. 2015.
- [11] C. Singhal and S. De, "Energy-efficient and QoE-aware TV broadcast in next-generation heterogeneous networks," *IEEE Commun. Mag.*, vol. 54, no. 12, pp. 142–150, Dec. 2016.
- [12] P. Unger and T. Kürner, "Modeling and performance analyses of hybrid cellular and broadcasting networks," *Int. J. Digit. Multimedia Broadcast.*, vol. 2009, Nov. 2009, Art. no. 329073.
- [13] K. Wang, Z. Chen, and H. Liu, "Push-based wireless converged networks for massive multimedia content delivery," *IEEE Trans. Wireless Commun.*, vol. 13, no. 5, pp. 2894–2905, May 2014.
- [14] A. Lykourgiotis, K. Birkos, T. Dagiuklas, E. Ekmekcioglu, S. Dogan, Y. Yildiz, I. Politis, G. O. Tanik, B. Demirtas, A. M. Kondo, and S. Kotsopoulos, "Hybrid broadcast and broadband networks convergence for immersive TV applications," *IEEE Wireless Commun.*, vol. 21, no. 3, pp. 62–69, Jun. 2014.
- [15] M. Crussière, C. Douillard, C. Gallard, M. Le Bot, B. Ros, A. Boutier, and A. Untersee, "A unified broadcast layer for horizon 2020 delivery of multimedia services," *IEEE Trans. Broadcast.*, vol. 60, no. 2, pp. 193–207, Jun. 2014.
- [16] Y. Wang, D. He, L. Ding, W. Zhang, W. Li, Y. Wu, N. Liu, and Y. Wang, "Media transmission by cooperation of cellular network and broadcasting network," *IEEE Trans. Broadcast.*, vol. 63, no. 3, pp. 571–576, Sep. 2017.
- [17] A. A. Razzac, S. E. Elayoubi, T. Chahed, and B. El Hassan, "Planning of mobile TV service in standalone and cooperative DVB-NGH AND LTE networks," in *Proc. 11th Int. Symp. Workshops Modeling Optim. Mobile, Ad Hoc Wireless Netw. (WiOpt)*, May 2013, pp. 609–614.
- [18] P. A. Fam, S. Paquelet, M. Crussière, J.-F. Hélar, and P. Brétillon, "Analytical derivation and optimization of a hybrid unicast-broadcast network for linear services," *IEEE Trans. Broadcast.*, vol. 62, no. 4, pp. 890–902, Dec. 2016.
- [19] H. Bawab, P. Mary, J.-F. Hélar, Y. Nasser, and O. Bazzi, "Global ergodic capacity closed-form expression of coexisting DVB-LTE-like systems," in *Proc. IEEE 79th Veh. Technol. Conf. (VTC Spring)*, May 2014, pp. 1–5.
- [20] A. Shokair, Y. Nasser, M. Crussière, J.-F. Hélar, and O. Bazzi, "Analytical study of the probability of coverage in hybrid broadcast-unicast networks," in *Proc. IEEE 29th Annu. Int. Symp. Personal, Indoor Mobile Radio Commun. (PIMRC)*, Sep. 2018, pp. 1–6.
- [21] M. Haenggi, *Stochastic Geometry for Wireless Networks*. Cambridge, U.K.: Cambridge Univ. Press, 2012.
- [22] M. Haenggi, J. G. Andrews, F. Baccelli, O. Dousse, and M. Franceschetti, "Stochastic geometry and random graphs for the analysis and design of wireless networks," *IEEE J. Sel. Areas Commun.*, vol. 27, no. 7, pp. 1029–1046, Sep. 2012.
- [23] I. Kaj, "Aspects of wireless network modeling based on Poisson point processes," in *Proc. Fields Inst. Workshop Appl. Probab.*, 2006, pp. 1–18.
- [24] W. Lu and M. Di Renzo, "Stochastic geometry modeling of cellular networks: Analysis, simulation and experimental validation," in *Proc. 18th ACM Int. Conf. Modeling, Anal. Simulation Wireless Mobile Syst.*, 2015, pp. 179–188.
- [25] J. G. Andrews, F. Baccelli, and R. K. Ganti, "A tractable approach to coverage and rate in cellular networks," *IEEE Trans. Commun.*, vol. 59, no. 11, pp. 3122–3134, Nov. 2011.
- [26] T. Kwon and H. Lee, "Broadcast range performances for random access-based wireless mutual broadcast," *IEEE Commun. Lett.*, vol. 22, no. 10, pp. 2108–2111, Oct. 2018.
- [27] P.-A. Fam, S. Paquelet, M. Crussière, J.-F. Hélar, and P. Brétillon, "Optimal capacity of hybrid unicast-broadcast networks for mobile TV services," in *Proc. IEEE Int. Symp. Broadband Multimedia Syst. Broadcast. (BMSB)*, Jun. 2016, pp. 1–5.
- [28] A. Ligeti, "Coverage probability estimation in single frequency networks in presence of correlated useful and interfering components," in *Proc. Gateway 21st Century Commun. Village. (VTC-Fall) IEEE VTS 50th Veh. Technol. Conf.*, vol. 4, Sep. 1999, pp. 2408–2412.
- [29] Z. Yazdanshenasan, H. S. Dhillon, M. Afshang, and P. H. J. Chong, "Poisson hole process: Theory and applications to wireless networks," *IEEE Trans. Wireless Commun.*, vol. 15, no. 11, pp. 7531–7546, Nov. 2016.
- [30] C.-H. Lee and M. Haenggi, "Interference and outage in Poisson cognitive networks," *IEEE Trans. Wireless Commun.*, vol. 11, no. 4, pp. 1392–1401, Apr. 2012.
- [31] I. M. Ryzhik and I. S. Gradshteyn, *Table of Integrals, Series, and Products*. New York, NY, USA: Academic, 1965.
- [32] *Frequency and Network Planning Aspects of DVB-T2*, EBU, UER, ITU, Geneva, Switzerland.



AHMAD SHOKAIR received the B.E. degree in communication and electronics engineering from Beirut Arab University (BAU), in 2013, and the master's degree in communication and signal processing from Lebanese University, Lebanon, in 2016. He is currently pursuing the Ph.D. degree in communication and networks with the Institute for Electronics and Telecommunications (IETR), National Institute of Applied Sciences (INSA), Rennes, France, in collaboration with Lebanese

University. His current research interests include mobile communication technologies, signal processing, and machine learning. He is currently involved in a project that includes cooperative wireless networks like broadcast/broadband hybridization.



MATTHIEU CRUSSIÈRE received the M.Sc. and Ph.D. degrees in electrical engineering from the National Institute of Applied Sciences (INSA), Rennes, France, in 2002 and 2005, respectively. In 2005, he joined the Department of Telecommunications and Electronic Engineering, INSA, as an Associate Professor and since 2005, he has been with the Digital Communication Department, Electronics and Telecommunications Institute of Rennes (IETR). He is currently the Head of the

SYSCOM Team, IETR. His current research interests include digital communications and signal processing techniques. His first works were focused on the optimization of high-bit rate power line communications using hybrid multicarrier and spread-spectrum waveforms. Then, he developed an expertise in adaptive resource allocation, optimization algorithms, and system design for multicarrier and multiantenna systems. During the last year, he applied his research results to the optimization of broadcast, broadband, and hybrid networks. In 2014, he started scientific collaborations as an Associate Researcher with the Institute of Research and Technology (IRT) B-COM in Rennes on large-scale antenna systems. He is the author or coauthor of more than 110 technical articles in international conferences and journals. He has been involved in several European and French national research projects in the field of powerline communications, broadcasting systems, and ultra wideband and mobile radio communications.



JEAN-FRANCOIS H ELARD received the Dipl.-Ing. and Ph.D. degrees in electronics and signal processing from the National Institute of Applied Sciences (INSA) in Rennes, in 1981 and 1992, respectively. From 1982 to 1997, he was a Research Engineer and then the Head of Channel Coding for the Digital Broadcasting Research Group, France Telecom Research Center (Orange Labs), Rennes. In 1997, he joined INSA Rennes, which is one of the Grandes Ecoles in France,

where he is currently a Full Professor, Classe Exceptionnelle, which is the highest rank. He was the Director of the Research of INSA Rennes during three years, from 2010 to 2013. During eight years, he was also the Deputy Director of the Rennes Institute for Electronics and Telecommunications (IETR, UMR CNRS 6164), which is an academic research laboratory of 400 people, created in 2002, in association with the CNRS. His current research interests include signal processing techniques for digital communications, such as space-time and channel coding, multicarrier modulation, and multiuser communications and cross-layer techniques. He involved in several European and national research projects in the fields of digital video terrestrial broadcasting, mobile radio communications and cellular networks, power-line and ultra-wide-band communications, cooperative communications, and relaying techniques. He is the author and coauthor of more than 300 technical articles in international scientific journals and conferences, and holds 15 European patents.



YOUSSEF NASSER received the Ph.D. degree from the National Polytechnic Institute of Grenoble, in 2006, and the HDR degree, in 2015. In 2003, he joined the Laboratory of Electronics and Information Technologies, Grenoble, where he involved in B3G and 4G systems. In 2007, he was a Research Engineer with INSA-Rennes and then joined the American University of Beirut (AUB), in 2010. His current research interests include signal processing on communications systems, 5G and 4G systems, and massive MIMO and localization. He has organized several international conferences and had been involved in the organization committees of IEEE flagship conferences (ICC, PIMRC, and SPAWC). He has proposed and has been involved in several research EU projects. He published more than 120 articles in top-tier journals and conferences.



OUSSAMA BAZZI received the B.E. degree in electrical engineering from the American University of Beirut (AUB), in 1987, and the master's and Ph.D. degrees in electronics from the University of Valenciennes and Hainaut Cambresis (UVHC), France, in 1988 and 1992, respectively. He joined Lebanese University, in 1996, where he is currently a Full Professor. He is currently the Head of the Research Group Telecoms, Signal Processing and Images (TSPI), Faculty of Sciences, Lebanese

University. His current research interests include signal processing and wireless and mobile radio communications. His current research projects include radio resource management, hybrid broadcast techniques, cooperative communication techniques, and cognitive radio networks.

...